USING FINITE-DIFFERENCE TIME-DOMAIN METHODS TO MODEL SONAR DATA IN COMPLEX ENVIRONMENTS

G R Elston and J M Bell

Department of Computing and Electrical Engineering, Heriot-Watt University, Edinburgh EH14 4AS

ABSTRACT

With continuing and rapid advances in computational power, the use of finite difference techniques for modeling complex problems becomes increasingly feasible. One such situation is the active sonar process. In this instance the aim is to model the entire process from pulse transmission, through propagation and scattering, to reception, thus producing realistic synthetic sonar signals and images.

The finite difference method is well suited to this application since the technique inherently models most aspects of the problem, and therefore provides many advantages over other techniques (such as ray tracing) which have previously been used for sonar simulation. The paper will present the initial developments of a finite difference model for the simulation of sonar signals which permits the inclusion of a distributed source, phase information, variable sound speed, multiple reflections and complex seabeds. Initial results obtained using the method illustrate each of these aspects.

1. INTRODUCTION

High frequency sonar image generation involves many subtle processes while the sound pulse is propagating through the water and interacting with the environment. These include refraction due to a variable sound speed within the water column; multiple scattering and reflection as a result of roughness on many scales at the sea surface and seabed, as well as from objects on and under the seabed and in the water; along with various sources of noise. One method of understanding the influence of each of these aspects on the resulting signals and images is computer simulation. This allows controlled experiments to be performed in which most of the complex environment is held constant, while the feature of interest is varied. An added benefit is that simulated data is inherently "ground-truthed".

In order to apply numerical modeling to a complex real-world problem such as the sonar process, simplifying assumptions are usually necessary to make the problem tractable. Different modeling methods (e.g. modes, wavenumber integration, ray tracing [1]) impose different assumptions and limitations on the complexity of the environments that can be accurately modeled, and on the types of output available from the simulation.

Motivated by the ray-based sidescan sonar simulation work by Bell [2], this work aims to produce a more general sonar simulator which is capable of modeling the entire sonar process and producing synthetic sonar signals and images. However, unlike the ray-based model, the aim is to be able to model accurately any high frequency active sonar system. The Finite-Difference Time-Domain (FDTD) method [3] has been chosen instead of ray tracing to allow general and complex scenes to be modeled. As will be discussed in section 2, it imposes the fewest limiting assumptions on the simulation, and gives the pressure field at the transducers as the output. However, this is at the expense of limited range and high computational overhead.

This paper demonstrates that several complex aspects of the problem can be simulated using a FDTD approach, and discusses methods for the future evolution of an FDTD general sonar model, including techniques to extend the range and reduce the computation time of the FDTD simulation.

2. THE FINITE-DIFFERENCE TIME-DOMAIN METHOD

The Finite-Difference Time-Domain method is based upon the discretisation of the governing differential wave equation (which functions in continuous space-time) to give approximate difference equations which operate on a finite, discrete, spatial and temporal grid. These difference equations relate the solution (for pressure and any other variables that are included in the particular scheme, e.g. particle velocity, density, stress, etc.) at one point to that at neighbouring points, and are applied everywhere on the spatial grid at consecutive time steps.

2.1 Theory

Several finite difference schemes are described in the literature [4, 5, 6, 7, 8], with different variables included depending on the application. In principle, the approximation can be made to any order of accuracy, commonly second order in time and second or fourth order in space. In this study, a second order (in both time and space) scheme has been used for the initial investigation of the technique. This scheme solves the wave equation for the acoustic pressure field, p. Applying the second order approximation to a 2-D environment gives the following recurrence relation [3, 6]:

$$p_{i,j}^{n+1} = r^2(p_{i-1,j}^n + p_{i+1,j}^n + p_{i,j-1}^n + p_{i,j+1}^n) + 2(1-2r^2)p_{i,j}^n - p_{i,j}^{n-1} \tag{1}$$

where the mesh ratio (involving the sound speed, c):

$$r = c\frac{\Delta t}{\Delta x} \tag{2}$$

and $p_{i,j}^{n+1} = p(i\Delta x, j\Delta y, n\Delta t)$ is the pressure as a function of range, depth and time step $i\Delta x$, $j\Delta y$ and $n\Delta t$, respectively (this assumes that the spatial discretisation is the same in each direction, i.e. $\Delta x = \Delta y$). Manipulation of the sound speed c in equation (2), and hence of the mesh ratio r, allows the introduction of a variable sound speed profile (SSP) within the water column.

In order for equation (1) to accurately model wave motion, the discretisation of continuous space-time must be at sub-wavelength (and period) resolution. The exact number of points per wavelength (PPW) and period (PPP) required depends on the particular scene being modeled, and is generally accepted to be at least 10 [3]. A further restriction is that this scheme is only conditionally stable. Applying Von Neumann stability analysis to equation (1) leads to the Courant-Freidrichs-Lewy (CFL) condition [6] for the mesh ratio (in the 2-D case):

$$r \leq \frac{1}{\sqrt{2}} \tag{3}$$

This imposes limits on the possible values of Δx, Δy and Δt in order that equation (1) remains stable. For any value of r above this limit, the errors in the approximation grow exponentially and rapidly dominate the solution.

2.1.1 Envelope detection. The end result of the FDTD simulation is a time-series signal at each transducer element of the model sonar array. A variety of signal processing techniques can then be applied to these signals. This is the reason the FDTD method can be used for a general sonar model: the signals received at each element can be obtained and then beam-formed as appropriate for the desired sonar type. In the results presented in section 3, simple envelope detection has been applied using a Hilbert transform [9]

2.2 Advantages

The primary advantage of the FDTD method is that it directly solves the wave equation in the time domain, therefore the signal at the transducers is obtained immediately as a time series without requiring any complex post-processing (which is the case with the ray model). Also, many complex effects are inherent to the model, including multiple reflections and scattering, inhomogeneous material parameters, boundaries with arbitrary geometry and wave phenomena (such as refraction and diffraction). In addition, it allows the inclusion of multiple sources and receivers (i.e. sonar arrays), user-defined input signals (e.g. CW, pulsed or chirped signals), and the controlled introduction of noise.

In the FDTD method the pressure field is known everywhere at all times throughout the simulation, hence the model can be used for any sonar geometry, mono- or bi-static, with stationary or moving arrays. Realistic transmit-beam patterns can also be simulated by using the same signals and transducer geometry as in the system being modeled. This flexibility gives the model the potential to simulate a wide variety of situations.

2.3 Disadvantage

The typical high frequency (>10 kHz) sonar applications of interest cover dimensions of the order of thousands of wavelengths in range and depth. With the fine discretisation required by the FDTD method (typically a few tens of PPW), the problem becomes extremely large, even in 2-D. For example, at 75 kHz ($\lambda \simeq 0.02$ m, i.e. 50λ/m) and 20PPW, a region 100m in range and 20m deep requires 50 million grid points. Given that the recurrence relation in equation (1) utilises three time steps simultaneously, the memory requirement for this region is 600MB, and it would take $\sim 300{,}000$ time steps for two-way propagation. This represents the emission and reception of only one pulse in 2-D; expanding to 3-D would lead to an increase in memory requirement and run time of several orders of magnitude.

However, this size of problem is becoming more feasible as the cost of large memory, multi-processor computers decreases, while their power is increasing rapidly. The algorithm is highly amenable to parallel processing because the same operation is being applied to every grid point, so the full space grid can be shared equally between all available processors. Several further options exist for decreasing the size of the problem, and these will be discussed in section 4.1.

3. RESULTS

To demonstrate the advantages of the FDTD method, many of the features discussed in section 2.2 will be illustrated. First, a simple reference example is presented which simulates a single point source in water with a constant SSP and flat surfaces. Multiple sources, a variable SSP, and a fractal rough seabed will then be added to show the capability of the method to model the increased complexity of the acoustic field and therefore of the received signals. The examples given all use a mesh density of 20PPW which, for the example above, is equivalent to a discretisation of about 1 mm in both range and depth. In order to maintain the stability of the algorithm, this requires a time discretisation of $\sim 0.5\,\mu$s. In each of the following simulations a shaped pulse (a sinusoid with a logistic function envelope) of eight periods was emitted from the transducer(s).

A pressure release ($p = 0$) boundary condition is employed at the boundaries, which is valid at the sea surface. At the seabed, the aim was to ensure that the FDTD method remained stable in the vicinity of a rough boundary, so a realistic shape (a fractal) was implemented as a first step. The pressure release boundary condition was also used here because it is very simple to implement. This allowed the effect of a

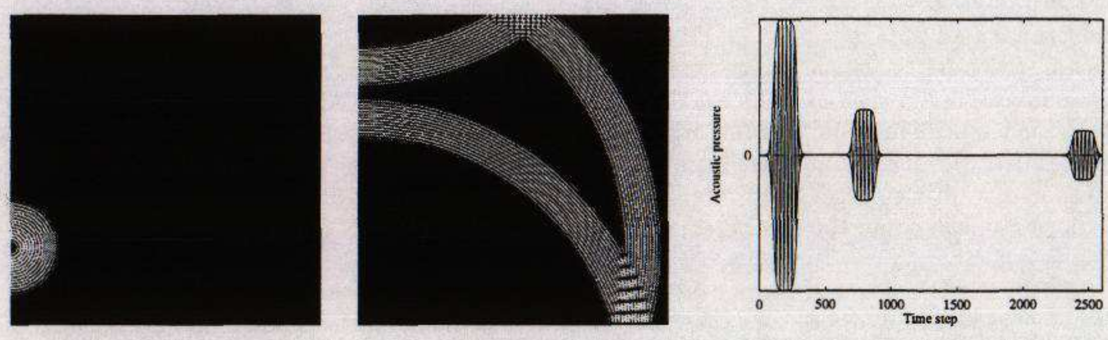

(a) $t/\Delta t = 250$ (b) $t/\Delta t = 1500$ (c) Received signal and envelope

Figure 1: Simple simulation scene – a point source in constant SSP water between flat surfaces.

rough surface shape on pulse reflection to be investigated, before attempting to apply a realistic boundary condition. On-going work (as discussed in section 4.1) aims to remove this simplifying assumption.

Much of the interesting data in the acoustic field is an order of magnitude or two lower in peak pressure than the dominant pulse. As this data would be almost invisible in an unmodified gray-scale image, the acoustic field images presented in this section have their lower intensities amplified to improve the contrast and increase the visibility of this data. However, it should be noted that the time domain signals have not been altered in any way; the plots are the direct results of the simulations. The pressure-magnitude images in this section display zero acoustic pressure as black, with white being the highest (absolute) pressure.

3.1 Reference solution

For a single point source located just above a flat perfectly-reflecting seabed in water with a constant sound speed, circular propagation (in 2-D) and mirror reflection are expected. These features are demonstrated in figure 1. This shows the acoustic pressure field in the 2-D slice of water at two different times (the time step is denoted by $t/\Delta t$); shortly after pulse transmission and then after reflection from both the seabed and the sea surface. The upper and lower surfaces coincide with the top and bottom of the images, but the vertical edges of the numerical grid are beyond the sides of the images.

The time series signal at a point mid-way between the source and the flat seabed is plotted in figure 1(c). This point was chosen so that the outgoing and the bottom- and surface-reflected pulses would be clearly visible in the same plot. It is evident that there is no acoustic energy between the direct reflections, as would be expected from mirror-flat surfaces. Spreading losses account for the pressure reduction over time.

3.2 Sonar array

The simple example above can then be extended by replacing the single source with a sonar array. This array is positioned far enough from the boundaries to prevent reflections during the time of interest. In figure 2, nine equally spaced source points in a vertical line, each emitting the same pulse, generate the expected beam pattern. The main lobe can be seen to propagate horizontally with lower intensity side lobes diverging from it, as anticipated.

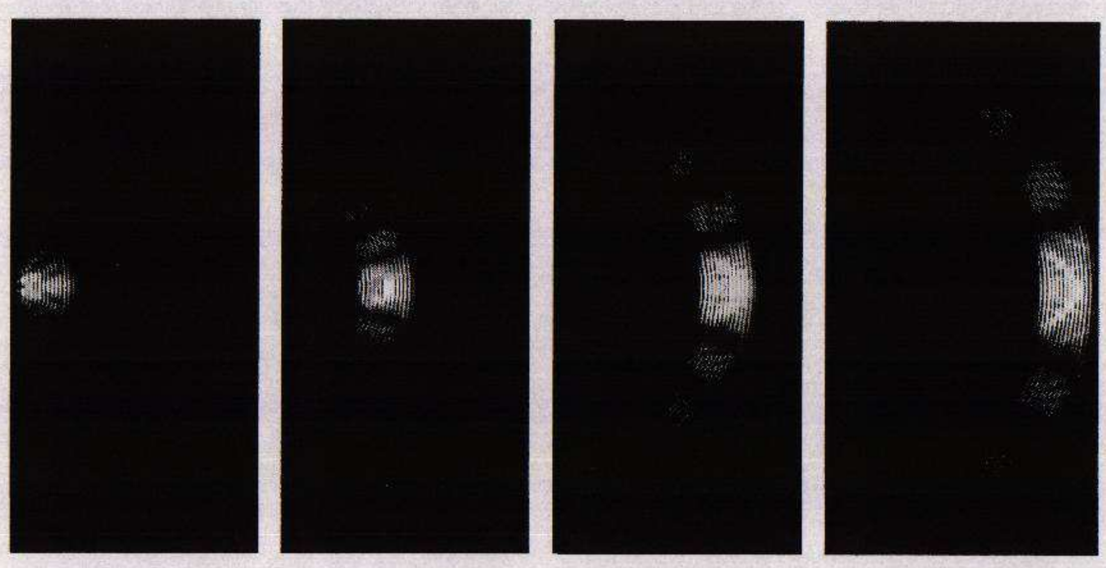

(a) $t/\Delta t = 250$ (b) $t/\Delta t = 500$ (c) $t/\Delta t = 750$ (d) $t/\Delta t = 1000$

Figure 2: Beam pattern obtained from a vertical array of nine point sources in an isovelocity medium.

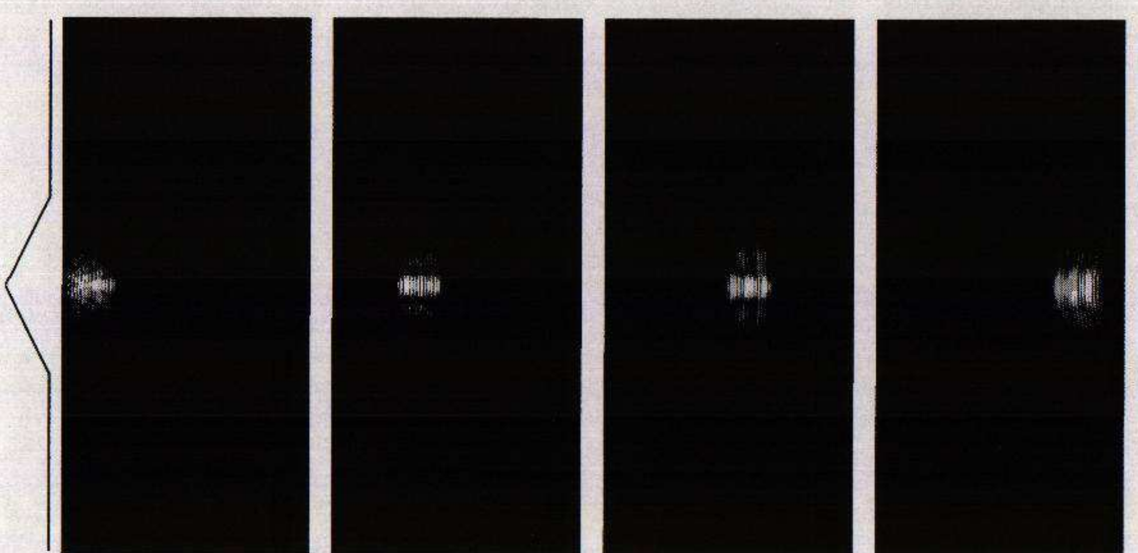

(a) $t/\Delta t = 250$ (b) $t/\Delta t = 500$ (c) $t/\Delta t = 750$ (d) $t/\Delta t = 1000$

Figure 3: Sound pulse trapped in a convergent sound channel (SSP shown at left).

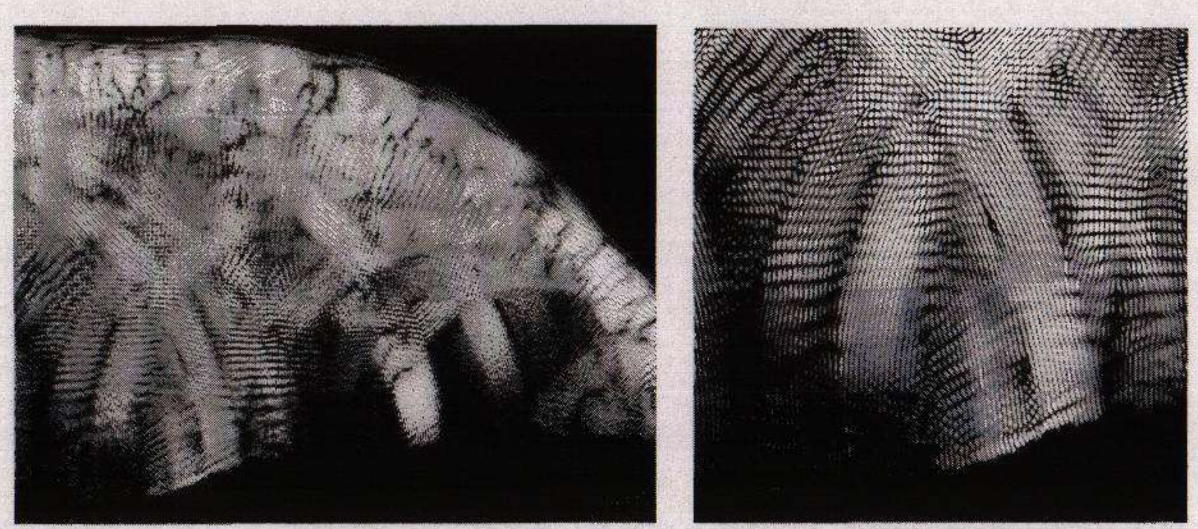

(a) $t/\Delta t = 4000$ (b) Enlarged view

Figure 4: Acoustic field after interaction with a rough (fractal) seabed.

3.3 Sound channel

To demonstrate that the FDTD method can include a variable sound speed in the water column, rather than the simple isovelocity case of the previous examples, figure 3 illustrates the effect of a converging sound channel centred on the sonar array. The sound speed in the simulation is altered via the mesh ratio of equation (1), and the SSP is also illustrated. The main lobe is clearly retained within the channel, and the side lobes can be seen to refract towards it. Interference and signal strengthening are also apparent.

3.4 Fractal rough seabed

The previous examples have considered a simple flat surface as a first approximation to a seabed. However, it is the energy back-scattered from the rough interface at the seabed that typically provides the detail in sonar images. This rough surface scattering creates an enormous amount of complexity in the acoustic field. The FDTD model allows any synthetic seabed to be incorporated, but a realistic shape is required in order to simulate this phenomenon successfully. Fractals have been found to be a good representation of seabed roughness over scales from centimetre to kilometre resolution [10] and provide a complex yet controlled surface suitable for this purpose. In this example, a seabed with a fractal dimension representative of natural seabeds has been quantised over a depth of 20 wavelengths and provides sub-wavelength roughness as well as larger scale bathymetry.

Figure 4 shows the resulting intricacy of the acoustic field due to the rough seabed. The images required log-normalisation and histogram equalisation in order to reveal the full complexity of this field. The source point is at the centre of the left-hand edge of figure 4(a), and the top left corner of the expanded view shown in figure 4(b). Regions of coherence exist within the field, along with complex regions of incoherence, and circular wavefronts appear to be the result of point-like scattering from prominent peaks in the seabed.

The received signal and envelope is again plotted for a receiver vertically below the source, mid-way to

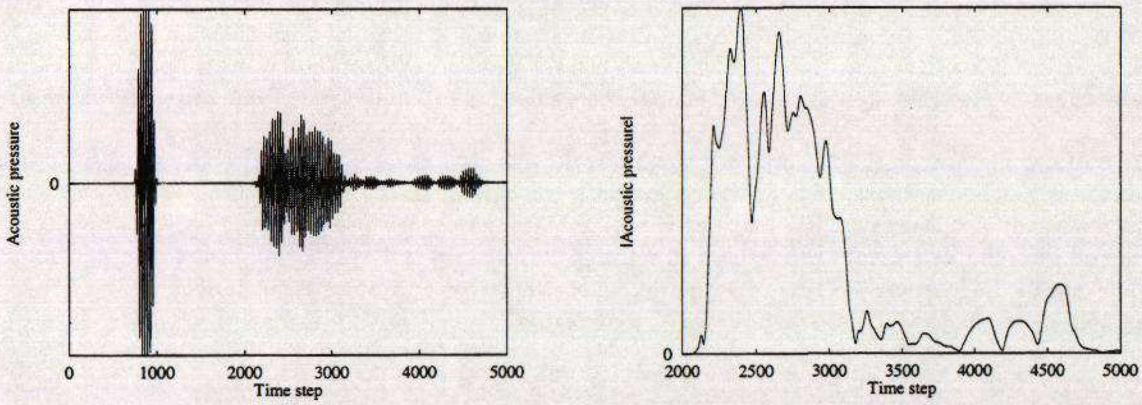

(a) Received signal

(b) Enlarged view of backscatter envelope.

Figure 5: Received signal and envelope at a point mid-way below the source.

the seabed (see figure 5). By comparing this signal to that in figure 1(c), it can be seen that a significant amount of energy is received after the initial echo, due to backscattering/reflection from the rough seabed. The shape of this received signal is complex, reflecting the roughness of the fractal seabed on many scales. It is this received signal envelope that produces sonar images, e.g. one line of a sidescan image. Many such one-line simulations of neighbouring regions of a 2-D seabed can be stacked up to produce a "pseudo" sidescan image in "$2\frac{1}{2}$-D".

4. CONCLUSIONS

The results presented in section 3 demonstrate the feasibility and significant potential of the FDTD approach for active sonar simulation. It allows realistic scenes to be modeled with little restriction on the shape or position of boundaries and objects, with many of the complex aspects of the problem being inherent to the model. The output of the simulation directly replicates that of actual sonar systems: a time series signal at each individual transducer of the sonar array.

4.1 Future Work

In order to produce a system capable of simulating realistic scenes in reasonable times, several improvements are required. The first is to add absorbing boundaries to the edges of the grid using the Perfectly Matched Layer (PML) [11, 12]. This will prevent reflections due to grid truncation and allow the area being simulated to be limited to the area of interest, rather than being confined to using a grid large enough to accommodate the spreading pulse in its entirety. Realistic seabed boundary conditions, with partial reflection – and thus partial transmission – and absorption will also be investigated.

The most important obstacle to overcome is the time it takes to run the FD simulation. The code is most efficient when the whole scene to be modeled is stored in core memory, however using the FD scheme described in section 2.1, this could take gigabytes. This is because of the relatively large number of points per wavelength required to keep equation (1) stable and accurate. Higher order FD schemes [4] remain stable and accurate with coarser numerical grids, and will thus reduce the amount of memory required for a particular scene (or, equivalently, allow a larger scene to be modeled with the same amount of memory). Coarser grids accelerate the simulation in two further ways: they contain fewer grid points to be calculated; and the time step is longer, thus fewer time steps are needed to simulate the same propagation time/distance.

A uniform mesh density (as employed in the work presented in section 3) is relatively easy to implement, but may not be the most efficient use of computer resources. In the water column, where the acoustic field is essentially propagating without great change or interaction, fewer PPW are needed; whereas near rough boundaries and/or changes in material properties, a finer grid is necessary to ensure accuracy and stability. The use of tiled regions will be investigated where the most appropriate mesh density and FD scheme are chosen depending on the characteristics of that region.

Once the fully functional system has been developed, it will be verified by comparing it to other models and benchmarks. Further verification may be needed to test areas not covered by other models. The model can potentially be used for many types of numerical experiment, including simulations of real scenes using ground-truthed data sets, once the goal of full 3-D simulation has been acheived.

ACKNOWLEDGEMENTS

The authors wish to acknowledge the support of DERA Bincleaves and EPSRC for this work.

REFERENCES

[1] M. J. Buckingham. Ocean-acoustic propagation models. *J. Acoustique*, 3:223–287, June 1992.

[2] J. M. Bell and L. M. Linnett. Simulation and analysis of synthetic sidescan sonar images. *IEE Proc. Radar Sonar and Navigation*, 144(4):219–226, 1997.

[3] F. B. Jensen, W. A. Kuperman, M. B. Porter, and H. Schmidt. *Computational Ocean Acoustics.* AIP Press, 1994.

[4] M. A. Dablain. The application of high-order differencing to the scalar wave equation. *Geophysics*, 51(1):54–66, 1986.

[5] A. R. Levander. Fourth-order finite-difference P-SV seismograms. *Geophysics*, 53(11):1425–1436, 1988.

[6] A. R. Mitchell and D. F. Griffiths. *The Finite Difference Method in Partial Differential Equations.* John Wiley & Sons, 1980.

[7] G. D. Smith. *Numerical Solutions of Partial Difference Equations: Finite Difference Methods.* Oxford University Press, 1985.

[8] J. Virieux. P-SV wave propagation in heterogeneous media: Velocity-stress finite-difference method. *Geophysics*, 51(4):889–901, 1986.

[9] J. G. Proakis and D. G. Manolakis. *Digital Signal Processing – Principles, Algorithms, and Applications.* Prentice-Hall, 1996.

[10] K. B. Briggs. Microtopographical roughness of shallow-water continental shelves. *IEEE J. Oceanic Eng.*, 14(4):360–367, 1989.

[11] J.-P. Berenger. A Perfectly Matched Layer for the Absorption of Electromagnetic Waves. *J. Computational Physics*, 114:185–200, 1994.

[12] Q.-H. Liu and J. Tao. The perfectly matched layer for acoustic waves in absorptive media. *J. Acoust. Soc. Am.*, 102(4):2072–2082, 1997.